Supplementary information

Self-assembling a natural small molecular inhibitor that shows aggregation-induced emission and potentiates antitumor efficacy

*Xiaona Chen,[a] Zhen Hu,[a] Liqian Zhou,[a] Fu Zhang,[a] Jianqin Wan,[a] Hangxiang Wang[a,]**

[a] *The First Affiliated Hospital; Key Laboratory of Combined Multi-Organ Transplantation, Ministry of Public Health, School of Medicine, Zhejiang University, Hangzhou, 310003, PR China.*

Corresponding Author: *Hangxiang Wang, The First Affiliated Hospital, School of Medicine, Zhejiang University; 79, Qingchun Road, Hangzhou 310003, China. Phone: +86-571-88208173; Fax: +86-571-88208173; E-mail: wanghx@zju.edu.cn*

EXPERIMENTAL SECTION

Materials

Dasatinib (DAS) was purchased from MedChemExpress (MCE; Shanghai, China). Thirteen inhibitors, namely, lenvatinib, golvatinib, resminostat, rapamycin, tacrolimus, cyclopamine, sorafenib, tasquinimod, imatinib, sunitinib, erlotinib, regorafenib, and sirtinol, were purchased from Selleck Chemicals (Shanghai, China). The bicinchoninic acid (BCA) protein assay kit was obtained from Fdbio science (Hangzhou, China). Quinine sulfate dihydrate for fluorescence analysis was purchased from Aladdin (Shanghai, China) and used as received. Transwell chamber (8.0 μm pore size) and BD Matrigel were purchased from Corning Inc. (USA). Dialysis membranes with a molecular weight cut-off of 2 kDa were obtained from Shanghai Yuanju Bio-Technology Co., Ltd. (Shanghai, China). Poly(ethyleneglycol)-*block*-poly($_{D,L}$-lactic acid) copolymers (PEG_{5k}-PLA_{8k}) were customized by Jinan Daigang Biomaterial Co., Ltd. (Shandong, China). LysoTracker Green DND-26 was obtained from Life Technologies (USA). Deionized (DI) water (18.2 MΩ·cm) was obtained with a Milli-Q system (Millipore, USA).

Preparation of supramolecular nanoparticles

The **s**elf-assembled **D**AS **N**ano**P**articles (termed **sDNPs**) were prepared using a reprecipitation protocol. Briefly, DAS (10 mg) was dissolved in dimethyl sulfoxide (DMSO, 1 mL), and the solution was quickly injected into deionized water (9 mL) under ultrasonication. Prior to the use, the solution was further dialyzed against DI water to remove DMSO. The concentrations of DAS were determined by analytical high-performance liquid chromatography (HPLC).

To fabricate nanosuspensions self-assembled from other molecular inhibitors, a similar procedure was carried out. Briefly, inhibitors (2 mg) were dissolved in DMSO (0.2 mL), followed by an identical reprecipitation protocol, to produce nanosuspensions at a concentration of 1 mg/mL.

Preparation of free DAS solutions for the *in vitro* use

To prepare the solutions containing free DAS for the *in vitro* experiments, a stock solution of DAS in DMSO was slowly injected into the cell culture media and then blended by pipetting to give a transparent solution.

Characterization of nanoparticles

The hydrodynamic diameters (D_H) and zeta potentials of self-assembled nanoparticles were determined by dynamic light scattering (DLS) on a Malvern Nano-ZS90 instrument (Malvern Instruments, Malvern, UK) at 25°C. The morphology of **sDNPs** was observed under a scanning electron microscope (Nova Nano 450, Thermo FEI) at 5 kV. Briefly, one drop of the **sDNP** solution was placed on a 200-mesh carbon-coated copper grid at room temperature. After drying for 15 min, the sample was observed.

Protein adsorption assay

To evaluate protein adsorption of **sDNPs**, three types of conventional formulations were included for comparison. For this purpose, EndoTAG-1 liposomes, PEGylated liposomes and polymeric micelles composed of poly(ethylene glycol)-block-poly($_{D,L}$-lactic acid) (e.g., PEG_{5k}-PLA_{8k}) (see the compositions in Table S2) were prepared according to the reported procedures.[1-3] The sizes and zeta potentials of the resulting formulations were determined on a Malvern Nano-ZS90 instrument. The solutions containing different formulations were incubated with bovine serum

albumin (BSA) or fetal bovine serum (FBS) for 30 min and then were centrifuged at 50,000 g for 60 min to obtain the precipitated particles and the supernatant. Adsorbed proteins in the precipitates and non-adsorbed proteins in the supernatant were determined by the BCA assay according to the manufacture's instruction and the standard sodium dodecyl sulphate-polyacrylamide gel electrophoresis (SDS-PAGE).

Evaluation of drug ratios in nanoaggregated state or in free drug form

To quantify the drug ratios in nanoaggregated state or in free drug form, two methods (i.e., ultrafiltration and ultracentrifugation) were use. For the ultrafiltration method, the **sDNPs** solution (600 μL) was centrifuged using an ultrafiltration centrifuge tube (molecular weight cut-off of 30 kDa) at 3000 g for 30 min. The DAS agents in free drug form were filtrated and were determined by HPLC. Moreover, the DAS agents in the self-assembled nanoaggregates were also determined by HPLC.

For the ultracentrifugation method, the **sDNPs** solution (1 mL) was subjected to ultracentrifugation at 50,000 g for 60 min at 4°C. After centrifugation, the supernatant was carefully removed from the pellets. HPLC was used to determine the contents of DAS in the supernatant and in the pellets.

Determination of fluorescence quantum yield (φ_f)

Fluorescence quantum yield of **sDNPs** in aqueous solution was investigated using quinine sulfate in 1.0 M sulphuric acid (φ_f = 0.55, excitation wavelength of 365 nm) as standard according to the following equation[4]: $\varphi_s = \varphi_r \left(\frac{A_r}{A_s}\right) \left(\frac{I_s}{I_r}\right) \left(\frac{{n_s}^2}{{n_r}^2}\right)$, where φ_r and φ_s represent the fluorescence quantum yields of the standard and the samples, respectively. A_r and A_s represent the absorbance of the standard and the measured samples at the excitation wavelength, respectively. I_r and I_s represent the integrated

emission intensities of the standard and the samples, respectively. n_r and n_s represent the refractive indices of the corresponding solvents of the solutions, respectively.

Molecular dynamics (MD) simulation

The structure of DAS was optimized under B3LYP/6-31G* with the Gaussian09 package. After that, sixteen DAS molecules were initially packed randomly by PACKMOL in a cuboid box with a length of 10 Å.[5] Then, the mixture was neutralized by adding sodium/chlorine counter ions and solvated in a cuboid box of TIP3P water molecules with solvent layers 10 Å between the box edges and the solute surface.[6]

All MD simulations were performed using AMBER16. The AMBER GAFF force field was applied, and the SHAKE algorithm was used to restrict all covalent bonds involving hydrogen atoms, with a time step of 2 fs. The particle mesh Ewald (PME) method was employed to treat long-range electrostatic interactions. For each solvated system, two minimization steps were performed before the heating step. The first 4000 cycles of minimization were performed with all heavy atoms restrained with 50 kcal/(mol·Å2), whereas solvent molecules and hydrogen atoms were free to move. Then, nonrestrained minimization was carried out with 2,000 cycles of steepest descent minimization and 2,000 cycles of conjugated gradient minimization. Afterwards, the whole system was first heated from 0 K to 300 K in 50 ps using Langevin dynamics at a constant volume and then equilibrated for 400 ps at a constant pressure of 1 atm. A weak constraint of 10 kcal/(mol·Å2) was used to restrain all the heavy atoms during the heating steps. Periodic boundary dynamics simulations were carried out for the whole system under the NPT (P = 1 atm and T = 300 K) ensemble in the production step. In the production phase, a 50 ns simulation

was carried out. For the dihedral angle analysis of both single free DAS and its aggregate in each system, 2 independent 50 ns production MD simulations were conducted to obtain enough configurations for data collection. Here, the time step of Newton's motions in the equation was 2 fs. The configurations were stored at a time interval of 0.1-0.2 ns for the whole system. After collecting MD conformations, we calculated the distribution of representative dihedral angles labeled in Figure 1J as a time function.

Cell culture

The DU145 human prostate carcinoma cell line and the 4T1 murine breast cancer cell line were obtained from the cell bank of the Chinese Academy of Science (Shanghai, China). DU145 cells were maintained in Dulbecco's modified Eagle's medium (DMEM), while 4T1 cells were cultured in PRMI 1640 medium. All media were supplemented with 10% FBS, penicillin (100 units/mL) and streptomycin (100 μg/mL), and the cells were maintained in a humidified incubator at 37°C with 5% CO_2.

3-(4,5-Dimethylthiazol-2-yl)-2,5-diphenyltetrazolium bromide (MTT) assay

The viability of cells treated with different drugs was evaluated by the MTT assay in DU145 cells and 4T1 cells. The cells were seeded in 96-well plates (3000-5000 cells per well) and cultured at 37°C for 24 h to allow the cells to attach to the wells. The cells were then incubated with medium containing **sDNPs** or free DAS at different predetermined concentrations and incubated for another 48 h at 37°C. After incubation, the medium was removed, and 30 μL of the MTT solution (5 mg mL^{-1}) was subsequently added to each well for 4 h at 37°C. The medium was then discarded, after which the resultant formazan crystals were dissolved with 100 μL of DMSO.

The absorbance of each well was measured using a microplate reader (Multiskan FC, Thermo Fisher Scientific) at a wavelength of 490 nm. Independent experiments performed with 3 replicates were used to obtain the statistical mean and standard deviation.

Apoptosis analysis

Annexin V-fluorescein isothiocyanate (FITC)/propidium iodide (PI) apoptosis detection kit was used to evaluate the cell apoptosis rate following the manufacturer's instructions (DOJINDO, Shanghai, China). After exposure to **sDNPs** or free DAS for 24 h, DU145 and 4T1 cells were harvested. After washing with 1× PBS, the cells were stained with 5 μL of annexin V-FITC and 5 μL of PI mixture for 15 min in the dark. To quantify the apoptosis rate, annexin V-FITC/PI double-stained cells were subjected to flow cytometry analysis (Cytoflex S, Beckman, USA). The data were analyzed with the corresponding software (Cytoflex S, Beckman, USA).

Cellular uptake and imaging

The cellular uptake of **sDNPs** was examined using confocal laser scanning microscopy (CLSM). DU145 cells were seeded in 20 mm laser confocal dishes at a density of 1.5×10^5 cells per dish and incubated for 24 h. Subsequently, the culture medium was replaced with fresh medium containing **sDNPs** (40 μM). The medium was discarded at predetermined time points, and the cells were washed three times with 1× PBS. After that, cells were stained with LysoTracker Green (final concentration of 100 nM) to label endo/lysosomes for 30 min at 37°C. After washing, the cells were immediately observed using a confocal microscope (FV3000, Olympus, Japan). The images were further analyzed with ImageJ (NIH, USA).

Effect of endocytic inhibitors on cellular uptake

DU145 cells were seeded in 12-well plates at a density of 3.0×10^5 cells per well for 24-h culture. Next, the cells were pretreated with or without the endocytic inhibitors filipin (3 μg mL^{-1}), cytochalasin D (40 μM) or CPZ (1, 2, or 4 μg mL^{-1}) for 30 min. Then, the cells were treated with **sDNPs** (40 μM) for a 4-h incubation and harvested for flow cytometry analysis (DxFLEX, Beckman, USA). In each analysis, the cell number was at least 10,000 cells, and the data were analyzed with DxFLEX software (Beckman, USA).

***In vitro* cell migration and invasion assays**

To perform the cell migration assays, the upper chambers of the Transwells (24-well insert; pore size, 8 μm) were seeded with 5×10^5 4T1 cells. The cells were dispersed in FBS-free PRMI 1640 medium containing **sDNPs** or free DAS at different concentrations. As a control, cells incubated with FBS-free PRMI 1640 medium without drug treatment were used. The lower chambers were filled with 700 μL of PRMI 1640 medium supplemented with 20% FBS as a chemoattractant. After incubation for 24 h, the cells that migrated to the lower chambers were fixed with methanol solutions for 30 min. After staining with 0.1% (w/v) crystal violet solution, the cells were observed using a microscope (IX73, Olympus).

For the cell invasion assays, the upper chambers were coated with Matrigel (BD Biosciences) before cell seeding. Subsequently, the same protocol described for the migration assay was followed to examine cell invasion.

Assay of capillary tube formation in HUVECs

Early-passage (≤ 6) human umbilical vein endothelial cells (HUVECs, 2.5×10^4 cells/well) were added to 96-well culture plates that were coated with 30 μl of Matrigel (BD Biosciences). The cells were then coincubated with free DAS or **sDNPs**

(50, 100, or 200 nM) for 4 h at 37°C. Cells treated with DMSO (0.1% v/v) were used as a control. The formation of HUVEC capillary-like structures on Matrigel was observed and photographed under an optical microscope. The capillary tube length and the number of branch points were quantified using ImageJ in at least six random microscopic fields (magnification, 100×). The experiments were repeated three times.

Wound-healing assay

To investigate the inhibitory effect of **sDNPs** or free DAS on HUVEC migration, we carried out a scratch wound-healing assay. HUVECs were seeded in 96-well plates and cultured to 90−95% confluency. Then, the cells were scratched with sterile tips to generate wounds, followed by incubation with blank culture medium (control group) or culture medium containing **sDNPs** or free DAS (100 or 200 nM). After 24 h of incubation, the medium was discarded, and fresh medium was added. Wound healing in these groups was observed and evaluated under an optical microscope (IX73, Olympus) at different time points. The migration rate (%) was calculated using the following formula: [(width of the wounded area at 0 h – width of the wounded area at x h)/width of the wounded area at 0 h] ×100, where x = 24, 48, or 72.

Hemolysis assays

The hemolytic activity of **sDNPs** was evaluated according to our previously reported protocol. Briefly, fresh blood was collected and washed with PBS to prepare RBC suspensions at a density of 1×10^8 cells/mL. Then, 400 μL of RBC suspension was mixed with **sDNP** solutions at varying concentrations, followed by incubation at room temperature for 2 h. RBCs treated with 1% Triton X-100 and PBS solution were set as the positive control and negative control, respectively. The absorbance of the released hemoglobin in each group was measured with a microplate reader

(Thermo-Scientific, Multiskan FC, USA). The hemolysis rate (%) was calculated using the following formula: [(absorbance of treated sample – absorbance of negative control)/ (absorbance of positive control – absorbance of negative control)] ×100.

Animal experiment

Balb/c athymic nude mice (male, 4-5 weeks) and Balb/c mice (female, 4-5 weeks) were purchased from Shanghai Experimental Animal Center, Chinese Academy of Science, and housed at the animal facility of the Zhejiang Academy of Medical Sciences. All animal experiments were approved by the Institutional Animal Care and Use Committee of the First Affiliated Hospital, Zhejiang University School of Medicine. All mouse studies were conducted in compliance with the National Institutes of Health Guide for the Care and Use of Laboratory Animals.

***In vivo* antitumor study in the DU145 cell-derived xenograft mouse model**

Balb/c athymic nude mice were inoculated subcutaneously in the right flank region with 100 μL of a cell suspension (containing 1.0×10^6 DU145 cells, in PBS). When the tumor size reached 150-200 mm^3, the DU145 tumor-bearing mice were randomly divided into four groups (n = 5) and received various treatments as indicated: (1) intravenous injection of 100 μL of saline; (2) intragastric administration of 100 μL of DAS solution (15 mg/kg); (3) intragastric administration of 100 μL of DAS solution (30 mg/kg); and (4) intravenous injection of 100 μL of **sDNPs** suspension (15 mg/kg) every 2 days for a total of 5 doses. Each mouse was marked and followed individually throughout the experiment. Tumor volumes and mouse body weights were measured using a caliper and an electronic balance, respectively, every two days for 26 consecutive days. Tumor volume (V) was calculated as follows: $V\ (mm^3) = 1/2 \times \text{length (mm)} \times \text{width (mm)}^2$. Mice were sacrificed at the end of the

experiment, and the tumors of the mice were excised, photographed as well as weighted.

Treatment of orthotopic breast cancer and inhibitory effects on lung and liver metastasis

To assess anticancer efficacy against orthotopic breast cancer and antimetastasis effects, 100 μL of 4T1 murine breast cancer cell suspension (containing 1.0×10^5 cells dispersed in saline) was injected into the breast fat pads of the mice. When the tumors reached approximately 200 mm^3, the mice were randomly divided into five groups (n = 7) and treated with saline, free DAS, and **sDNPs** with the same dosing regimen used in the DU145-xenograft model. Each mouse was marked and followed individually throughout the whole experiment. Tumor volumes and mouse body weights were measured using a caliper and an electronic balance every 2 days for 12 consecutive days. Tumor volume (V) was calculated as follows: V (mm^3) = 1/2 × length (mm) × width $(mm)^2$. At the end point, the mice were sacrificed. The tumor, lung and liver tissues from each group were excised and photographed. Moreover, the lung and liver tissues from each group were assessed by histological examinations to detect metastatic lesions. Five fields were randomly chosen and imaged for analysis.

Histopathological analysis

The tumor tissues were excised 2 days after the final treatment with various drugs, fixed overnight with 4% formaldehyde, embedded in paraffin, and cut into 5-μm-thick slices. The sections were stained with hematoxylin and eosin (H&E, Sigma) to detect morphological changes. Apoptosis analysis was performed by the TUNEL assay with an *In Situ* Cell Death Detection Kit according to the manufacturer's protocol (Fluorescein, Roche Applied Science). To detect the proliferation of tumor

cells, Ki67-positive cells were detected with an antibody. The stained tumor slices were visualized using a microscope (IX73, Olympus) at 200× magnification. Five fields per tumor were randomly chosen and imaged for analysis.

Immunotoxicity test

ICR mice were divided into five groups (n = 3) and treated as indicated: (1) i.v. injection of 200 μL of saline; (2) i.v. injection of 200 μL of blank PEG_{5k}-PLA_{8k} NPs (270 mg/kg, 9-fold higher than the DAS dose); (3) i.v. injection of 200 μL of DAS@PEG_{5k}-PLA_{8k} NPs (at a DAS dose of 30 mg/kg and a polymer dose of 270 mg/kg); (4) i.g. administration of 200 μL of DAS solution (30 mg/kg); and (5) i.v. injection of 200 μL **sDNP** suspension (30 mg/kg) every 2 days for a total of 5 doses. At days 0, 1, 9, 18, and 30 post-administration, blood samples were collected, allowed to clot by leaving them undisturbed for 30 min and centrifuged at 1000 × g for 10 min. Then, the sera were collected, frozen and stored for further analysis of the concentrations of predetermined chemokines and cytokines. The samples were further thawed completely, mixed well and then centrifuged at 1000 × g for 10 min (4°C) prior to use. Twenty-five microliters of serum was diluted with the assay buffer (25 μL) provided in the LEGENDplexTM Multi-Analyte Flow Assay Kit (BioLegend Inc., USA). The standard curve method was applied by preparing serial dilutions of chemokine and cytokine standards in the matrix. Control serum, standards, and serum samples of animals subjected to various treatments were incubated with antibody-immobilized beads for 30 min and quantified with a flow cytometer according to the manufacturer's instructions (Cytoflex S, Beckman, USA).

Statistical analysis

The quantitative results are presented as the mean ± SD. Statistical significance was assessed using Student's *t*-test (SPSS statistics 17.0). A p-value < 0.05 was considered statistically significant, while a p-value < 0.01 was considered highly significant.

Table S1. Quantitative analysis of free DAS fraction in the solution of **sDNPs**.

Method	DAS assembled in aggregates (μg/mL) (percentage)	Free DAS (μg/mL) (percentage)
Ultrafiltration	1355.6 ± 67.9 (97.5% ± 0.2%)	35.2 ± 1.0 (2.5% ± 0.2%)
Ultracentrifugation	1411.9 ± 52.1 (96.4% ± 0.0%)	53.0 ± 1.6 (3.6% ± 0.0%)

Table S2. Compositions and characterization of three formulations.

Formulation	Compositions	Size (nm)	Zeta potential (mV)
EndoTAG-1 liposome	Paclitaxel, DOTAP, DOPC	277.4±17.7	32.97±0.45
PEGylated liposome	Paclitaxel, Egg-PC, Chol, DSPE-PEG_{2000}	143.8±5.0	-34.27±2.35
Paclitaxel@PEG_{5k}-PLA_{8k}	Paclitaxel, PEG_{5k}-PLA_{8k}	69.8±0.6	-0.12±0.86

Table S3. Characterization of nanoparticles formed by self-assembling thirteen molecular inhibitors measured by DLS.

Molecular Inhibitors	Particle size (nm)	PDI[b]
Lenvatinib[a]	353.00 ± 8.62	0.28 ± 0.02
Golvatinib	154.63 ± 6.69	0.33 ± 0.01
Resminostat	277.87 ± 38.54	0.16 ± 0.04
Rapamycin	165.77 ± 2.61	0.14 ± 0.02
Tacrolimus	444.57 ± 39.00	0.28 ± 0.04
Cyclopamine	173.77 ± 9.56	0.11 ± 0.03
Sorafenib	618.87 ± 20.14	0.25 ± 0.04
Tasquinimod	786.83 ± 67.38	0.06 ± 0.02
Imatinib	361.40 ± 70.85	0.64 ± 0.18
Sunitinib	749.27 ± 40.01	0.28 ± 0.07
Erlotinib	1057.60 ± 79.11	0.18 ± 0.11
Regorafenib	1456.67 ± 159.81	0.86 ± 0.04
Sirtinol	2872.00 ± 650.64	0.69 ± 0.54

[a)] All measurements were performed in triplicate;

[b)] PDI, polydisperse index

Table S4. Photophysical data of **sDNPs** in the mixture of DMSO/water (v/v, 1:99) and free DAS in DMSO using quinine sulfate as reference.

	λ_{Ex} (nm)	φ_f	α_{AIE}[a]
Quinine sulfate	365	0.55	--
Free DAS in DMSO	398	0.03	5.0
sDNPs	398	0.15	

[a)] AIE amplification factor ($\alpha_{AIE} = \varphi_{f,\ aggregation}/\varphi_{f,\ solution}$)

Table S5. *In vitro* cytotoxicity of **sDNPs** against DU145 and 4T1 cells after 48-h incubation. The cell viability was determined by the MTT assay, and the data were expressed as $IC_{50} \pm$ SD in nM.

Cell line	DU145	4T1
Free DAS	363.2	343.5
sDNPs	291.4	254.0
p[a]	0.005	0.013

[a] Statistical significance between cytotoxicity of free DAS and **sDNPs** in the same cell line using Student's *t*-test.

Supplementary Figures

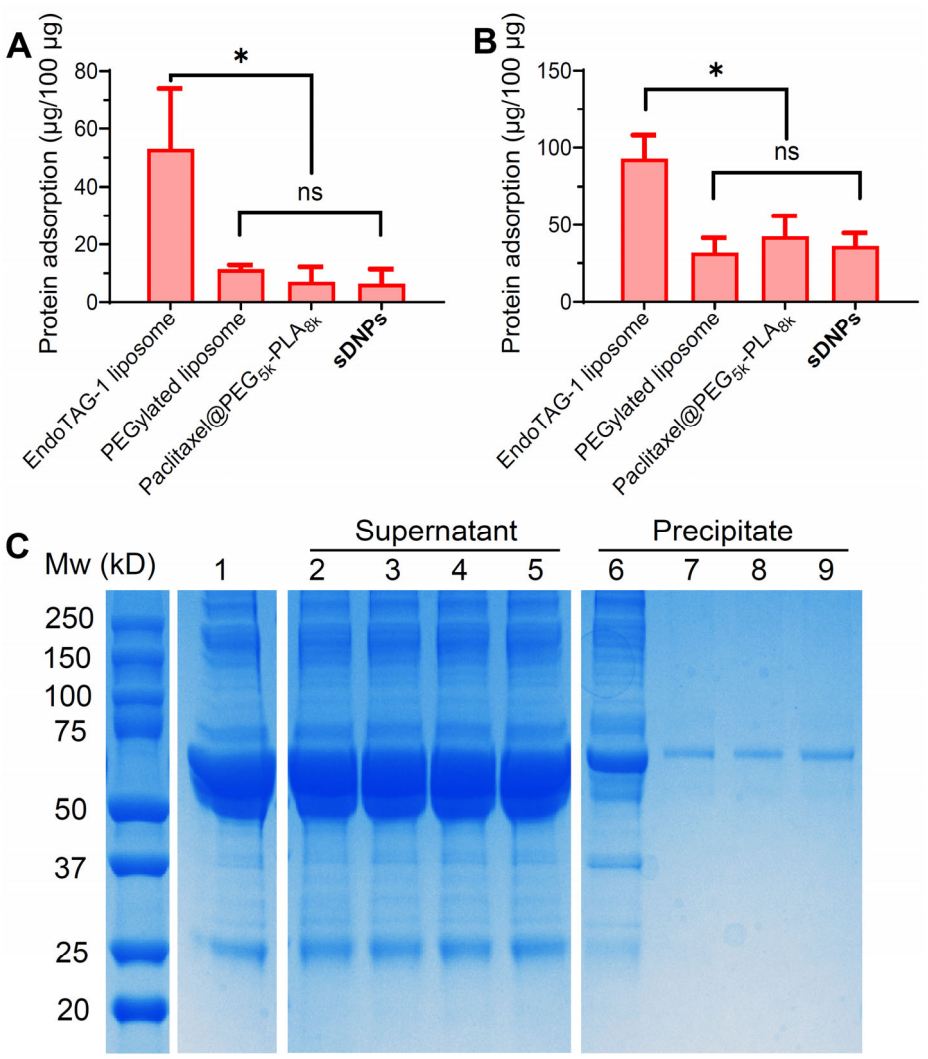

Figure S1. Protein adsorption on different formulations after 30-min incubation with (A) BSA and (B) serum. (C) 10% SDS-PAGE and Coomassie Brilliant Blue staining of the proteins adsorbed on the particles upon incubation with fetal bovine serum (FBS). Lane 1: FBS; lanes 2-5: non-adsorbed proteins in the supernatant from the samples of EndoTAG-1 liposomes, PEGylated liposomes and polymeric micelles (Paclitaxel@PEG_{5k}-PLA_{8k}), and **sDNPs**; lanes 6-9: adsorbed proteins on nanoparticles precipitated by centrifugation from the samples of EndoTAG-1 liposomes, PEGylated liposomes and polymeric micelles, and **sDNPs**. The data are presented as the mean ± SD (n = 3). * $p < 0.05$, ^{ns} $p > 0.05$.

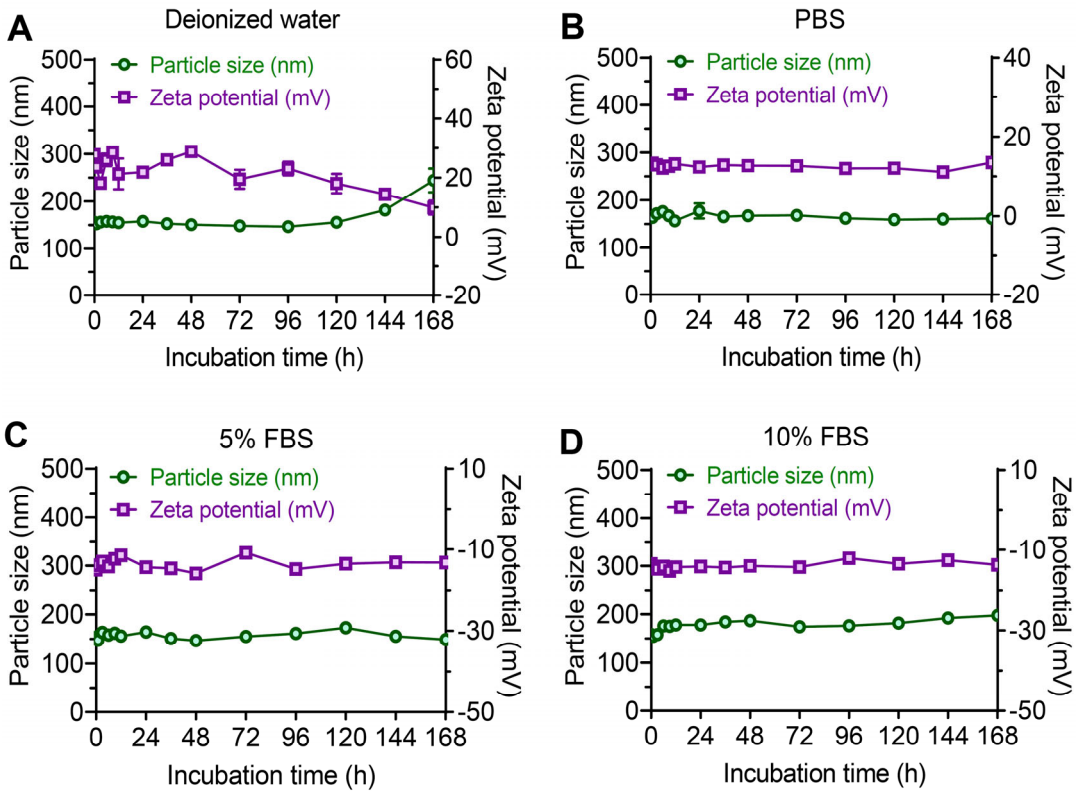

Figure S2. The colloidal stability of **sDNPs** in A) DI water, B) PBS (10 mM, pH7.4) and C, D) FBS (5 and 10%, v/v). The particle sizes and zeta potentials of **sDNPs** were measured by DLS over the time course of 7 days. The data are presented as the mean ± SD (n = 3).

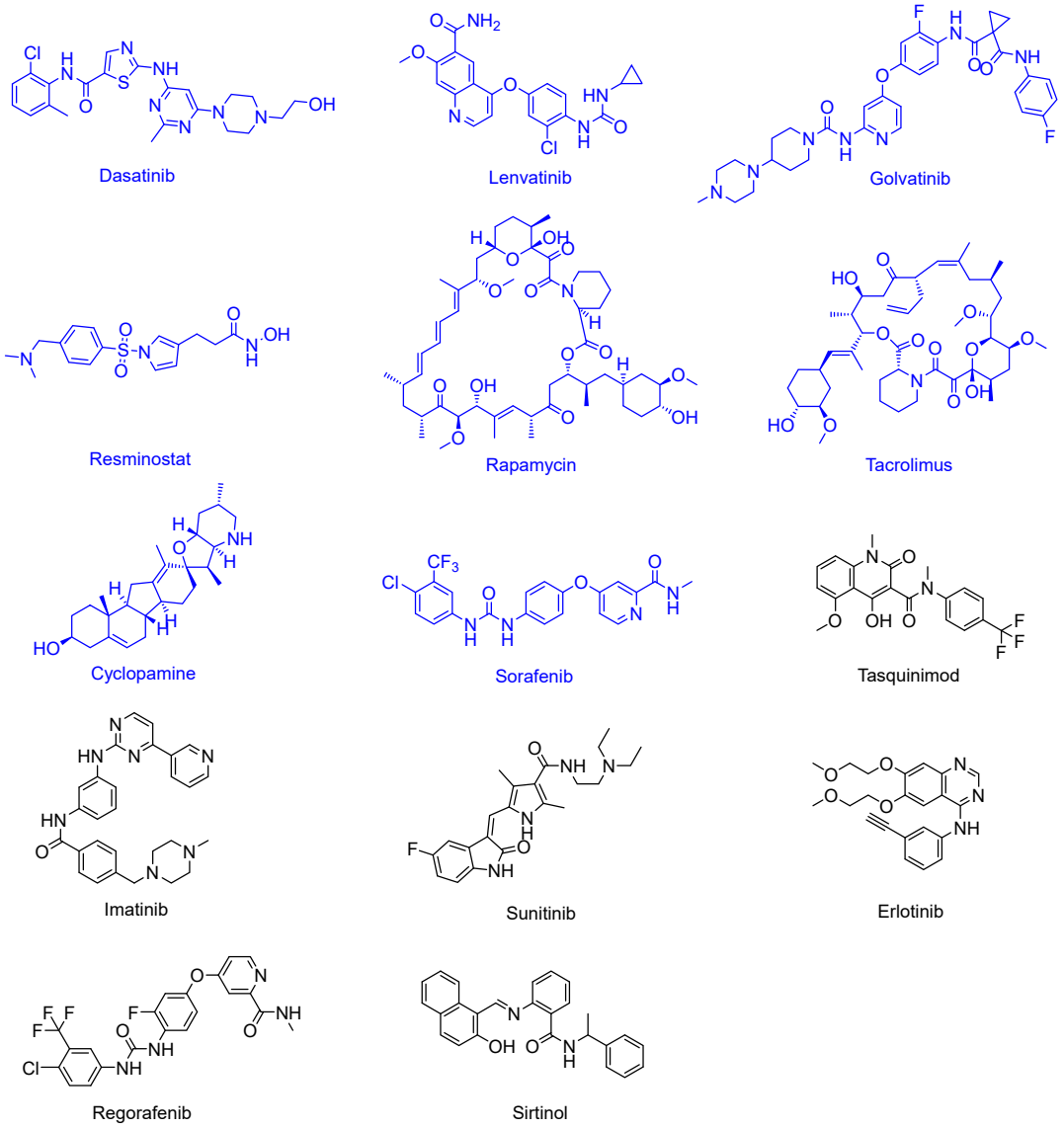

Figure S3. Chemical structures of fourteen molecular inhibitors used to screen for self-assembly behavior in this study.

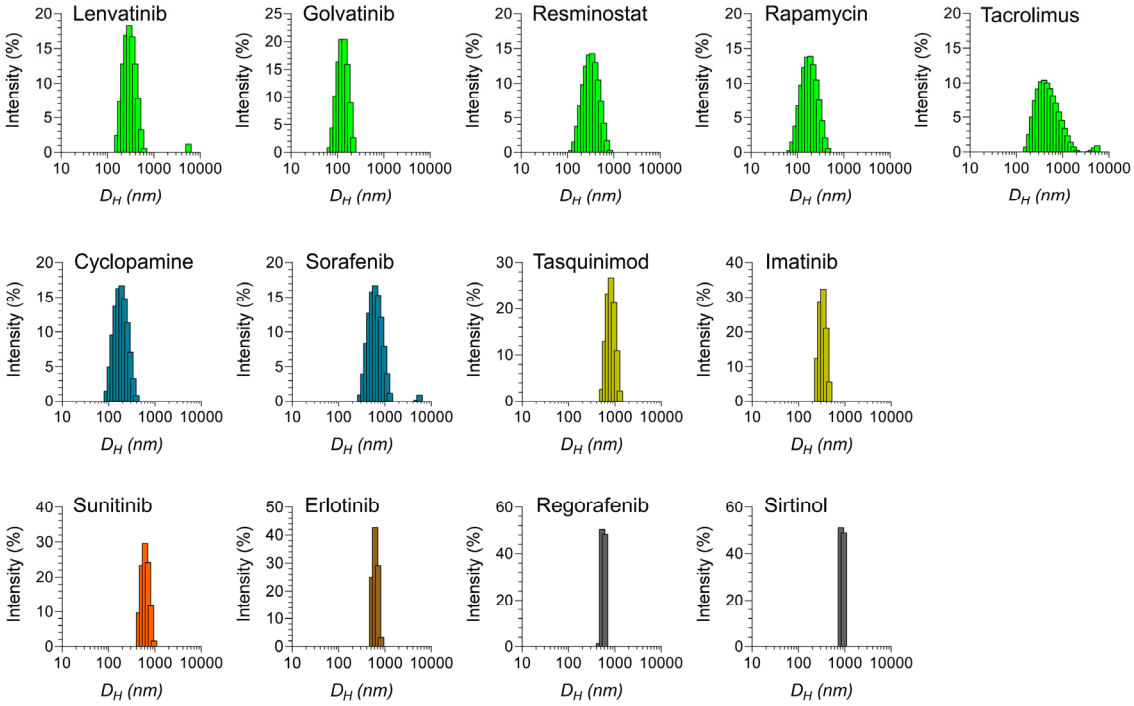

Figure S4. Aggregate formation by thirteen individual molecular inhibitors using a nanoprecipitation method without any excipients. Their size distributions were measured by dynamic light scattering (DLS). In all of the preparations, the final drug concentration was 1 mg/mL.

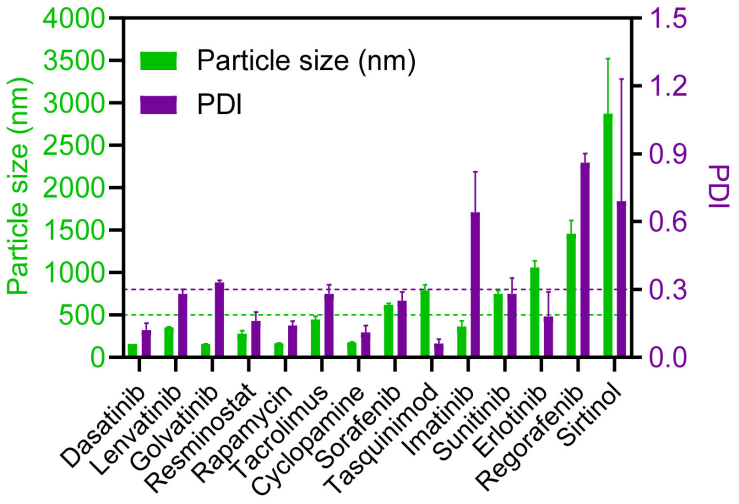

Figure S5. Hydrodynamic diameters (D_H) and polydispersity index (PDI) values of self-assembled drug nanoaggregates. The experiments were performed (n = 3) to evaluate their self-assembly behavior.

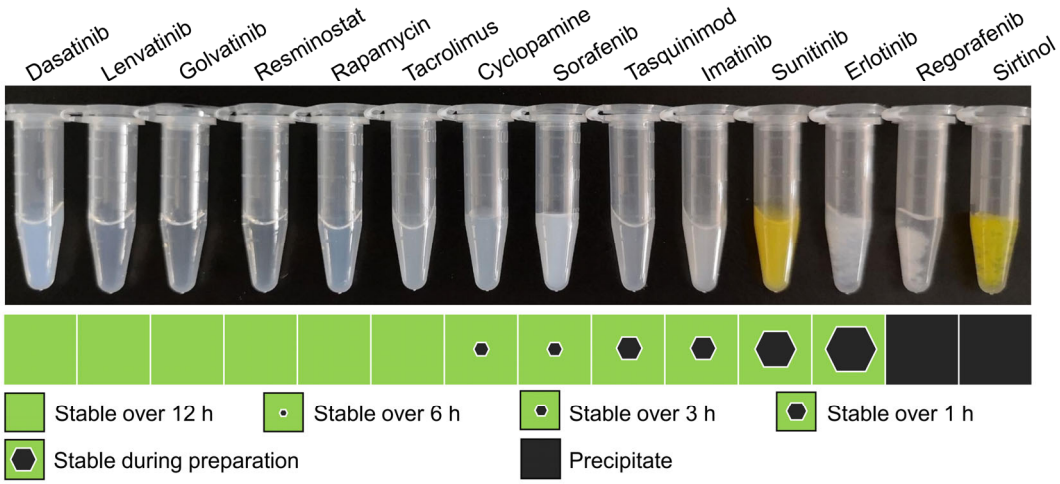

Figure S6. The stability test for aggregates. The water dispersions of aggregates after preparation were photographed. Precipitate formation was observed, and the time was recorded individually to assess stability.

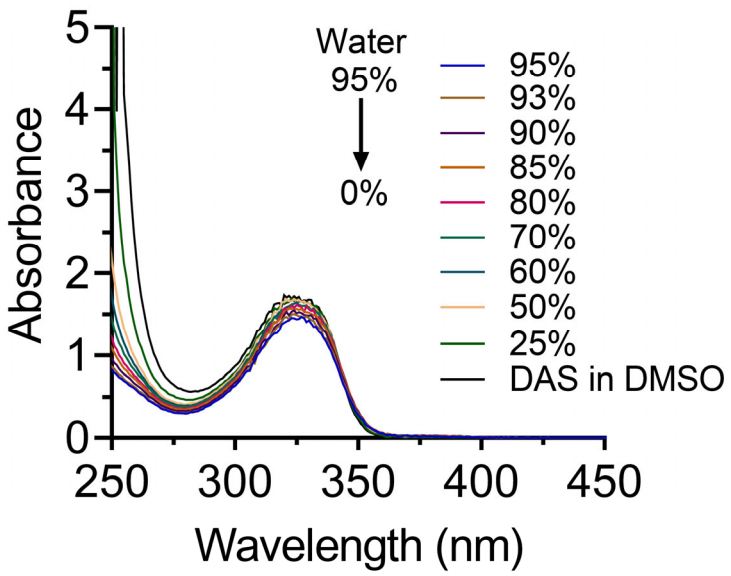

Figure S7. Absorption spectra of DAS in the DMSO/water mixtures with different water fractions (f_w).

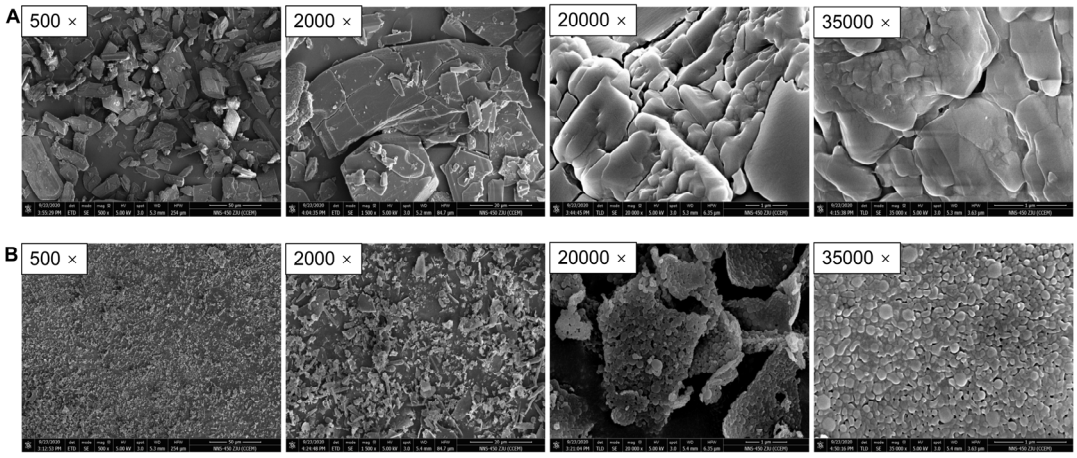

Figure S8. Scanning electron microscopy (SEM) images of the morphology of (A) the DAS powder and (B) lyophilized **sDNPs**.

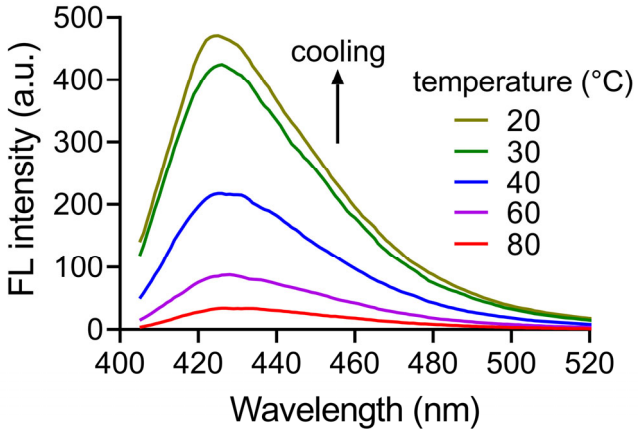

Figure S9. Fluorescence spectra of DAS at different temperatures. DAS was dissolved in DMSO at a final concentration of 50 mg/mL. Excitation wavelength: 398 nm.

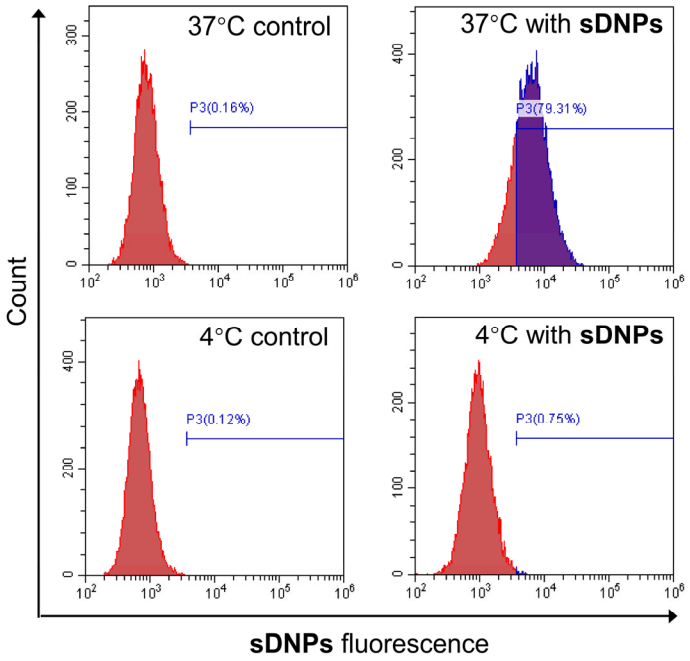

Figure S10. Effect of temperature on the internalization of **sDNPs**, as analyzed by FACS. **sDNPs** were added to DU145 cells preincubated at either 4 or 37°C. After 4 h of cell incubation at either temperature, the fluorescence intensity of untreated controls and cells exposed to **sDNPs** (at a concentration of 40 μM) was observed by flow cytometry. Excitation wavelength: 405 nm. Emission channel: 450 nm.

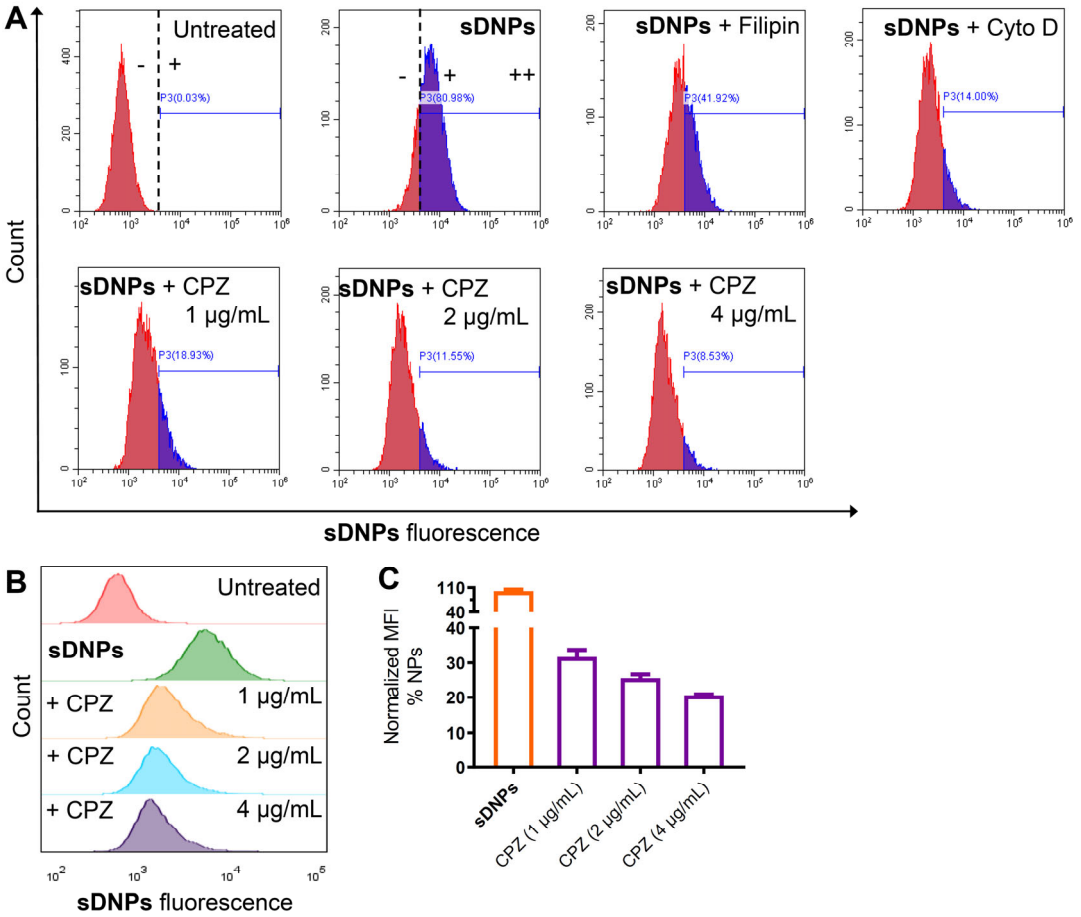

Figure S11. Cellular uptake of **sDNPs** in the presence of either inhibitor analyzed by FACS. **sDNPs** were added to cells that were preincubated with filipin (3 µg/mL), cytochalasin D (40 µM), or CPZ (1, 2, 4 µg/mL). (A) After 30 min of incubation with the inhibitor, the internalization of **sDNPs** over 4 h was analyzed by flow cytometry. (B, C) The cells incubated with **sDNPs** in the absence of inhibitors were set as the **sDNP** positive control, and all inhibitors decreased the internalization of **sDNPs** to varying degrees.

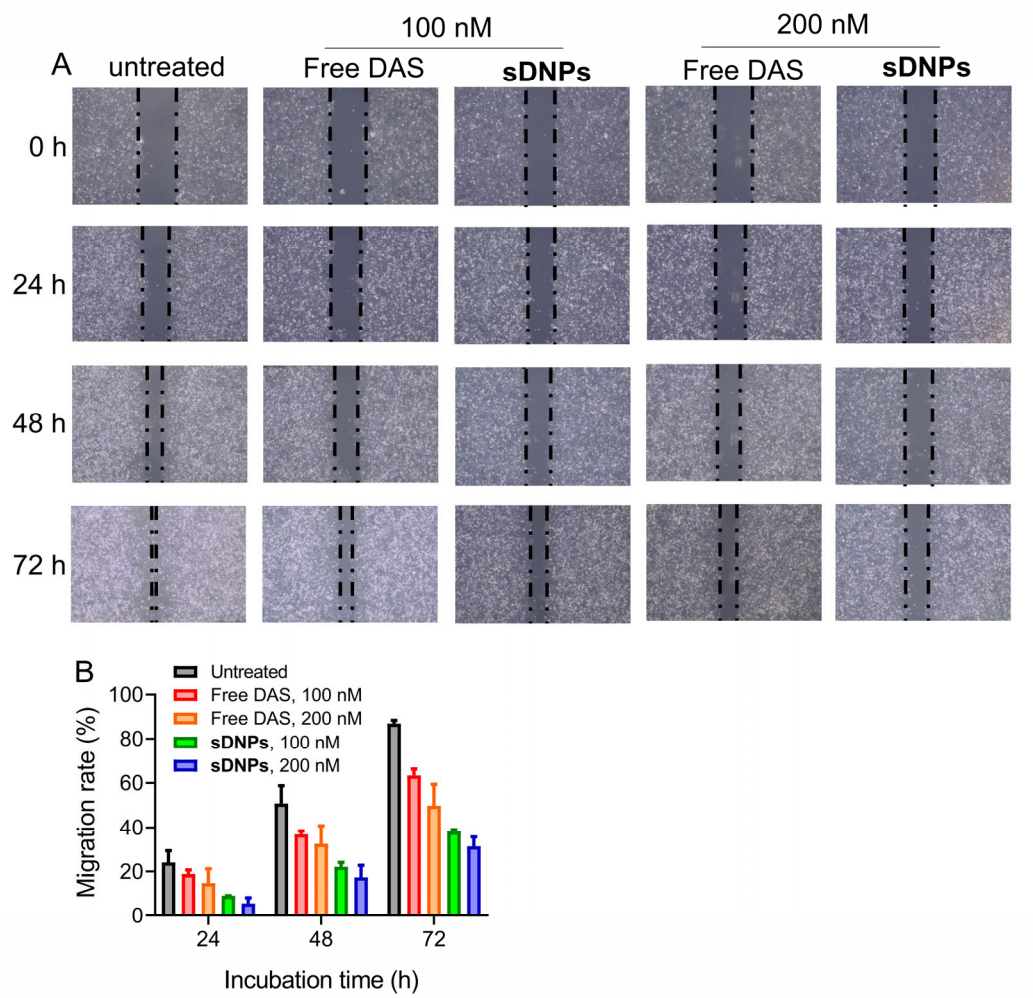

Figure S12. Wound-healing assay. After creating vertical wounds, the HUVECs were incubated with free DAS or **sDNPs** at DAS concentrations of 100 or 200 nM for 24 h. The untreated cells were used as a control. (A) The cells were photographed by microscopy after 0, 24, 48 and 72 h of incubation. (B) The widths of the wounded areas were measured to perform quantitative analysis. Each bar represents the mean ± SD of three independent experiments.

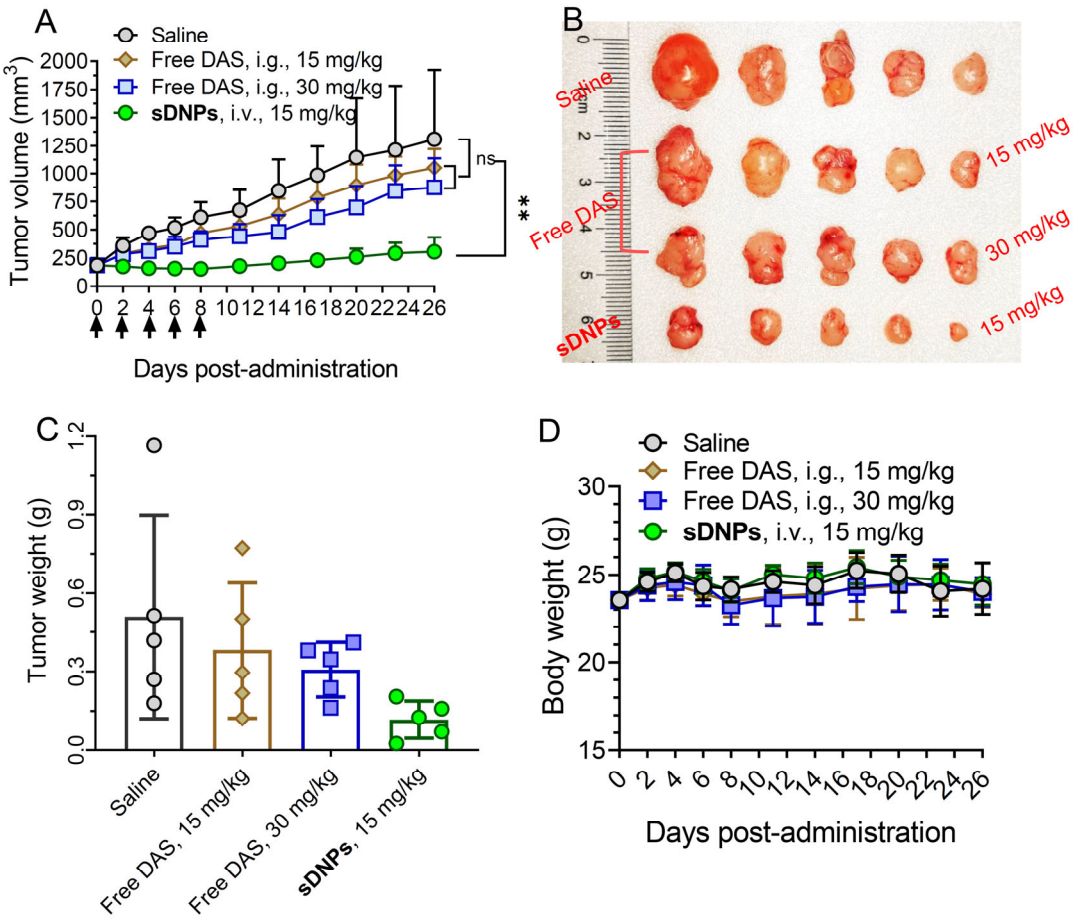

Figure S13. *In vivo* antitumor efficacy of **sDNPs** in the mice bearing human prostate DU145 xenografts. The mice were administered with drugs on days 0, 2, 4, 6, and 8. (A) Tumor growth was recorded every 2 days. Photograph (B) and weights (C) of excised tumors on day 26. (D) Mice body weights were recorded every 2 days. The data are presented as the mean ± SD (n = 5). ** $p < 0.01$, ^{ns} $p > 0.05$.

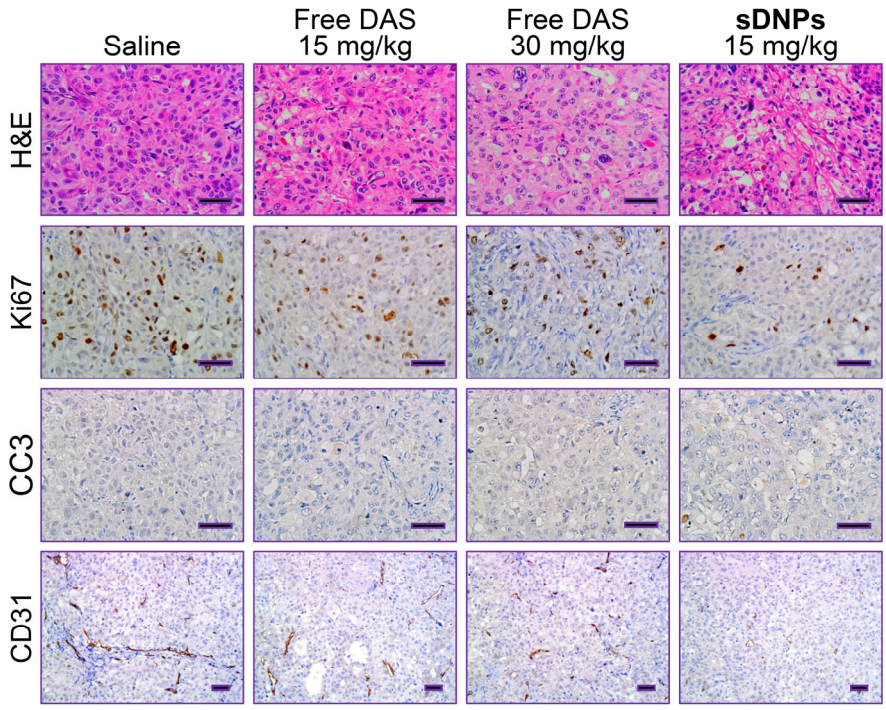

Figure S14. Representative images of the tumors with H&E, Ki67, CC3 and CD31 immunohistochemistry in the DU145-xenograft mouse model. Scale bars: 50 μm.

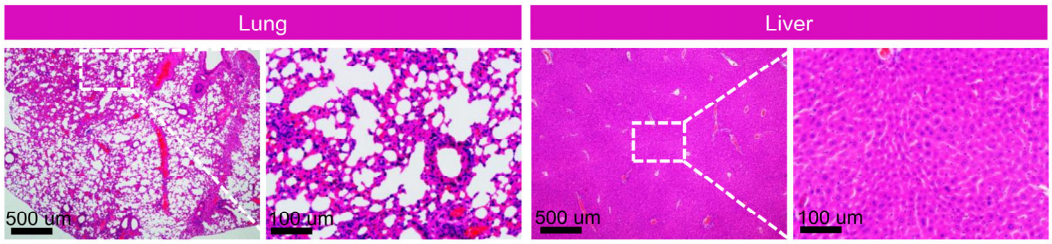

Figure S15. H&E staining of lungs and livers excised from healthy Balb/c mice. The images on the right show an enlargement of the region in the white rectangle.

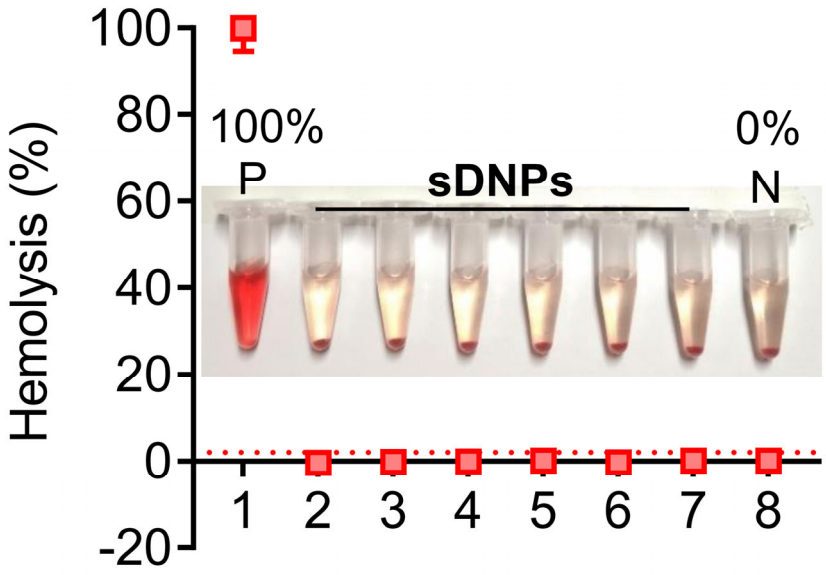

Figure S16. *In vitro* hemolysis assay. Relative hemolysis rates of RBC suspensions upon incubation with **sDNPs** at different concentrations. The tubes, from left to right, are the positive control (P, Triton X-100, set as 100%), 0.6, 0.5, 0.4, 0.3, 0.2, and 0.1 mg/mL **sDNPs**, and the negative control (N, PBS, set as 0%).

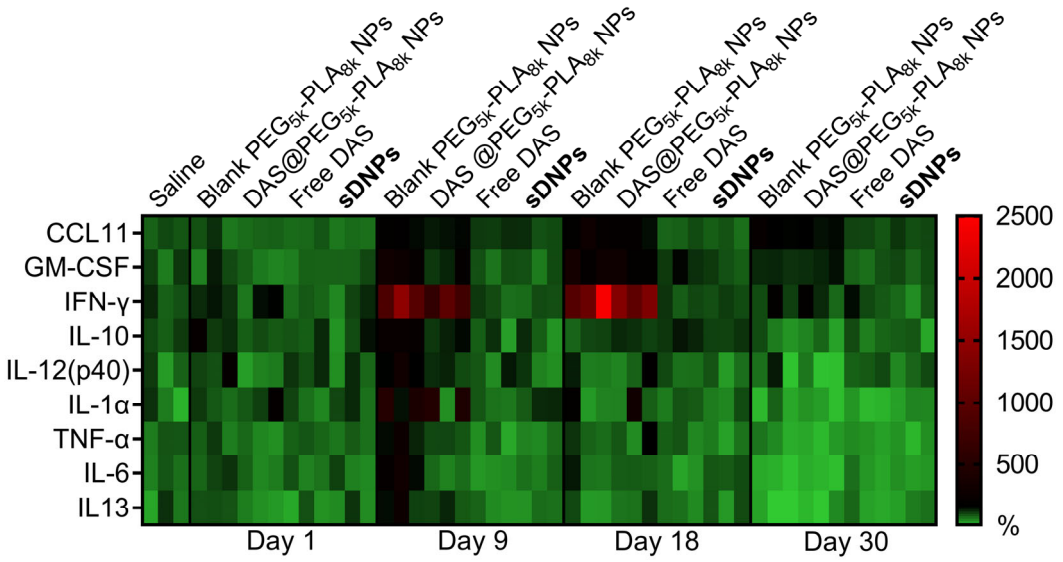

Figure S17. Heat map of the relative expression of cytokines and chemokines in mouse serum collected on days 0, 1, 9, 18 and 30 post-administration. The mice were injected with saline, blank PEG_{5k}-PLA_{8k} NPs, DAS@PEG_{5k}-PLA_{8k} NPs, free DAS or **sDNPs** *via* the tail vein (n = 3).

References

1. M. E. Eichhorn, I. Ischenko, S. Luedemann, S. Strieth, A. Papyan, A. Werner, H. Bohnenkamp, E. Guenzi, G. Preissler, U. Michaelis, K. W. Jauch, C. J. Bruns and M. Dellian, *Int. J. Cancer*, 2010, **126**, 1235-1245.
2. L. L. Shi, Y. C. Wang, Q. C. Wang, Z. N. Jiang, L. L. Ren, Y. P. Yan, Z. X. Liu, J. Q. Wan, L. L. Huang, B. N. Cen, W. D. Han and H. X. Wang, *J. Controlled Release*, 2020, **324**, 289-302.
3. J. Q. Wan, Y. T. Qiao, X. N. Chen, J. P. Wu, L. Q. Zhou, J. Zhang, S. J. Fang and H. X. Wang, *Adv. Funct. Mater.*, 2018, **28**.
4. H. S. Joshi, R. Jamshidi and Y. Tor, *Angew. Chem. Int. Ed.*, 1999, **38**, 2722-2725.
5. L. Martinez, R. Andrade, E. G. Birgin and J. M. Martinez, *J. Comput. Chem.*, 2009, **30**, 2157-2164.
6. L. P. Wang, K. A. McKiernan, J. Gomes, K. A. Beauchamp, T. Head-Gordon, J. E. Rice, W. C. Swope, T. J. Martinez and V. S. Pande, *J. Phys. Chem. B*, 2017, **121**, 4023-4039.